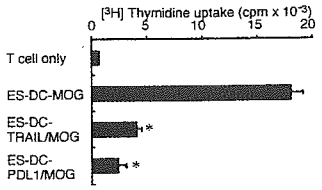

FIGURE 5. Decreased proliferative response to MOG peptide of MOG-reactive T cells cocultured with ES-DC expressing MOG plus TRAIL or MOG plus PD-L1. T cells (2×10^5) isolated from inguinal lymph nodes of CBF_1 mice immunized according to the protocol for EAE induction were cocultured with irradiated ES-DC-MOG, TRAIL/MOG, or PDL1/MOG (2×10^4) for 3 days, as in Fig. 4*A*. The asterisks indicate that the differences in responses are statistically significant ($p < 0.01$) compared with ES-DC-MOG. The data are each representative of three independent and reproducible experiments with similar results.

completely prevented by pretreatment with either of these genetically modified ES-DC. In contrast, pretreatment with ES-DC-MOG, ES-DC-TRAIL/OVA (as irrelevant Ag), or ES-DC-PDL1/OVA had no effect (Fig. 6*C* and Table II). Thus, the prevention depended on both the presentation of the MOG peptide and the expression of TRAIL or PD-L1 by ES-DC. If 2×10^6 of ES-DC-TRAIL/MOG or ES-DC-PDL1/MOG was given as a one-injection administration, EAE was similarly prevented (data not shown). However, if 5×10^5 of ES-DC-TRAIL/MOG or ES-DC-PDL1/MOG was used for one injection, the disease severity was not reduced (data not shown). Thus, $\sim 1 \times 10^6$ of genetically modified ES-DC as one-injection dose is apparently necessary for the prevention of EAE under this experimental condition.

We asked whether TRAIL or PD-L1 should be coexpressed by the same ES-DC as one presenting MOG peptide for their capacity to protect mice from EAE. As shown in Fig. 6*D* and Table II, coinjection of ES-DC-MOG together with ES-DC-TRAIL or ES-DC-PDL1 did not reduce the severity of EAE. Thus, coexpression of TRAIL or PD-L1 with MOG peptide by ES-DC is necessary for the protection from EAE. These results emphasize the advantage of the technology of ES cell-mediated genetic modification of DC, by which one can generate clonal transfectant DC carrying multiple expression vectors.

Next, we tested whether or not treatment with ES-DC after immunization with MOG would achieve some preventive effect on EAE. As shown in Fig. 7*A*, mice were immunized according to the protocol for EAE induction and, after that, injected with ES-DC on days 5, 9, and 13 (1×10^6 cells/mouse/injection). Even in this postimmunization treatment, injection of ES-DC-TRAIL/MOG or ES-DC-PDL1/MOG reduced severity of the disease, but ES-DC-MOG did not do so (Fig. 7*B* and Table II).

Decreased T cell response to MOG in mice treated with ES-DC-TRAIL/MOG or -PD-L1/MOG

We examined whether treatment with ES-DC-TRAIL/MOG or -PDL1/MOG would reduce the activation of MOG-specific T cells. Forty-two days after the immunization according to the protocol for EAE induction (Fig. 6*A*), we isolated inguinal lymph node cells and analyzed their proliferative response upon restimulation in vitro with MOG peptide. As shown in Fig. 8*A*, the magnitude of proliferation of lymph node cells isolated from mice treated with ES-DC-TRAIL/MOG or -PDL1/MOG was not increased in response to MOG peptide. In contrast, that of lymph node cells from ES-DC-MOG-treated or untreated mice was increased with statistical significance. In the presence of 25 μg/ml MOG peptide, stimulation index (count in the presence of MOG peptide/count in the absence of Ag) for that of untreated, ES-DC-MOG, -TRAIL/MOG, and -PDL1/MOG-treated mice were 2.8, 2.4, 1.3, and 1.0, respectively. These results suggest that treatment with ES-DC-TRAIL/MOG or -PDL1/MOG inhibited the activation of MOG-specific T cells or reduced their number in mice immunized with MOG peptide and adjuvants.

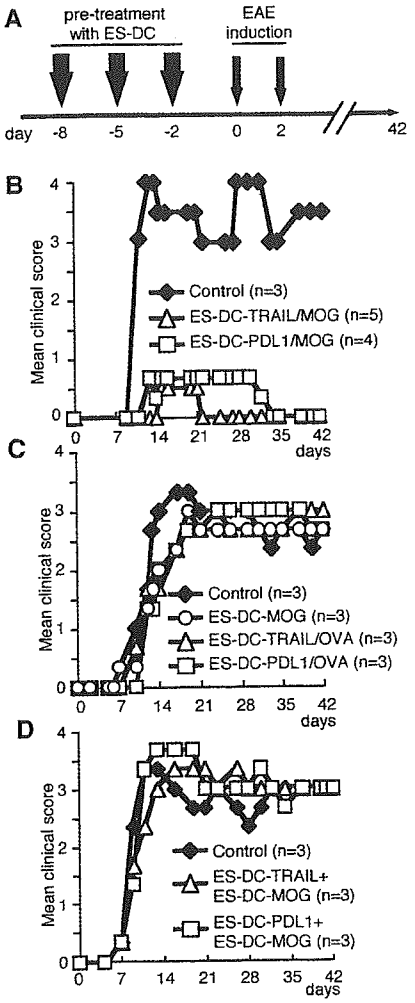

FIGURE 6. Prevention of MOG-induced EAE by pretreatment of mice with ES-DC expressing MOG plus TRAIL or MOG plus PD-L1. *A*, The schedule for pretreatment and induction of EAE is shown. CBF_1 mice (three to five mice per group) were i.p. injected with ES-DC (1×10^6 cells/injection/mouse) on days -8, -5, and -2. EAE was induced by s.c. injection of MOG peptide plus *M. tuberculosis* H37Ra emulsified in IFA on day 0, and i.p. injection of *B. pertussis* toxin on days 0 and 2. *B–D*, Disease severity of mice treated with ES-DC-TRAIL/MOG, ES-DC-PDL1/MOG, or RPMI 1640 medium (control) (*B*), ES-DC-MOG, ES-DC-TRAIL/OVA, ES-DC-PDL1/OVA, or RPMI 1640 medium (control) (*C*), coinjection with ES-DC-MOG plus ES-DC-TRAIL, ES-DC-MOG plus ES-DC-PDL1, or RPMI 1640 medium (control) (*D*) is shown. The data are each representative of at least two independent and reproducible experiments, and data of all experiments are summarized in Table II.

Next, we examined whether or not treatment with ES-DC would affect immune responses to an irrelevant exogenous Ag. We treated mice with ES-DC-MOG, -TRAIL/MOG, -PDL1/MOG, or RPMI 1640 medium (control) using the same schedule described above, and subsequently immunized the mice with KLH/CFA. Eleven days after the immunization, we isolated inguinal lymph

Table II. *Suppression of EAE induction in CBF$_1$ mice treated with ES-DC*[a]

Treatment (ES-DC)	Disease Incidence	Day of Onset	Mean Peak Clinical Score
No Treatment (control)	26/26	10.5 ± 1.1	3.3 ± 0.4
Pre[b]- TRAIL/MOG	**3/10**	18.3 ± 2.4	**0.3 ± 0.4**
Pre- PDL1/MOG	**5/10**	13.4 ± 2.1	**0.8 ± 0.8**
Pre- MOG	8/8	10.5 ± 1.3	3.0 ± 0.3
Pre- TRAIL/OVA	6/6	10.2 ± 2.9	3.0 ± 0
Pre- PDL1/OVA	6/6	11.3 ± 0.9	3.0 ± 0
Pre- TRAIL + MOG	6/6	10.2 ± 1.2	3.2 ± 0.6
Pre- PDL1 + MOG	6/6	10.2 ± 0.6	3.3 ± 0.7
Post[c]- TRAIL/MOG	**3/6**	18.7 ± 4.4	**0.5 ± 0.5**
Post- PDL1/MOG	**3/6**	13.7 ± 1.1	**1.0 ± 1.0**
Post- MOG	6/6	10.8 ± 1.0	3.2 ± 0.3

[a] Data are combined from a total of 10 separate experiments including those shown in Figs. 6 and 7. EAE was induced by s.c. injection at the tail base of a 0.2-ml IFA/PBS solution containing 400 μg of *M. tuberculosis* and 600 μg of MOG peptide once (on day 0), together with i.p. injections of 500 ng of purified *B. pertussis* toxin on days 0 and 2. For prevention of EAE, mice were injected i.p. with ES-DC (1×10^6 cells/mouse/injection) [b]on days −8, −5, and −2 (preimmunization treatment), or [c]on days 5, 9, and 13 (postimmunization treatment). The incidence and the clinical score reduced by ES-DC treatment are indicated in boldface.

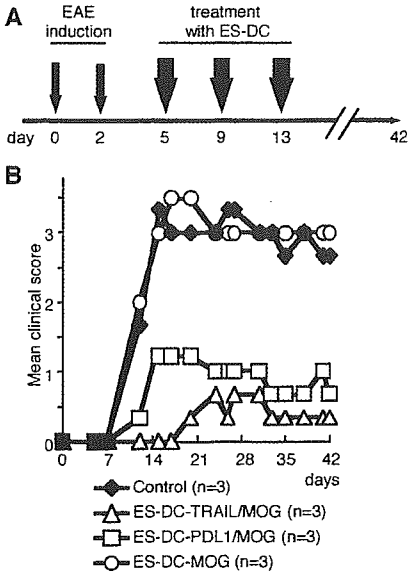

FIGURE 7. Inhibition of MOG-induced EAE by treatment with ES-DC expressing MOG plus TRAIL or MOG plus PD-L1 after immunization with MOG. *A*, The schedule for induction of EAE and treatment is shown. CBF$_1$ mice (three mice per group) were immunized on days 0 and 2 according to the EAE induction schedule described above, and subsequently i.p. injected with ES-DC (1×10^6 cells/injection/mouse) on days 5, 9, and 13. *B*, Disease severity of mice treated with ES-DC-TRAIL/MOG, ES-DC-PD-L1/MOG, ES-DC-MOG, or RPMI 1640 medium (control) is shown. The data are each representative of two independent and reproducible experiments, and data of all experiments are summarized in Table II.

node cells and analyzed their proliferative response upon restimulation with KLH in vitro. As a result, lymph node cells of ES-DC-treated and control mice showed the same magnitude of proliferative response (Fig. 8*B*), thereby indicating that the treatment with such genetically modified ES-DC did not affect the immune response to irrelevant Ags.

We immunohistochemically analyzed spinal cord, the target organ of the disease, of mice subjected to EAE induction with or without treatment with ES-DC. Massive infiltration of CD4$^+$ T cells, CD8$^+$ T cells, and Mac-1$^+$ macrophages was observed in spinal cords of untreated control mice (Fig. 9). In contrast, T cells and macrophages hardly infiltrated into the spinal cord of mice treated with ES-DC-TRAIL/MOG or ES-DC-PDL1/MOG. The results of histological analysis are in parallel with the severity of EAE and activation state of MOG-specific T cells of each mouse.

Increased number of apoptotic cells in splenic CD4$^+$ T cells by treatment with ES-DC-TRAIL/MOG

With regard to the mechanism of prevention of EAE by transfectant ES-DC, we analyzed the apoptosis of CD4$^+$ T cell in spleens of mice treated with ES-DC by staining with annexin V and subsequent flow-cytometric analysis. In the results, we observed that transfer of ES-DC-TRAIL/MOG caused an increase of apoptosis of CD4$^+$ T cells in recipient mice (17.3 ± 2.5%), compared with transfer of ES-DC-MOG (12.0 ± 0.4%), ES-DC-PDL1/MOG (12.2 ± 0.5%), or RPMI 1640 medium control (10.2 ± 0.8%). In the experiments, three mice were used for each group. Increased numbers of apoptotic cells in spleen of mice transferred with ES-DC-TRAIL/MOG were also observed in histological analysis with TUNEL staining (Fig. 10). The capacity of ES-DC-TRAIL/MOG to cause apoptosis of T cells may play some role in the protection from EAE.

Discussion

DC are the most potent APC responsible for priming of naive T cells in initiation of the immune response. Recent studies revealed that DC are also involved in the maintenance of immunological self-tolerance, promoting T cells with regulatory functions, or inducing anergy of T cells. In vivo transfer of Ag-loaded DC with a tolerogenic character is regarded as a promising therapeutic means to negatively manipulate immune response in an Ag-specific manner. Various culture procedures used to generate DC with a tolerogenic character have been reported (31–36). Mouse bone marrow-derived DC generated in the presence of IL-10 and/or TGF-β or in the low dose of GM-CSF showed immature phenotypes, a low-level expression of cell surface MHC and costimulatory molecules, and induced T cell anergy in vitro and tolerance to specific Ags or allogeneic transplanted organs in vivo. In humans, monocyte-derived immature DC loaded with antigenic peptides and transferred in vivo have been shown to cause the Ag-specific immune suppression (37).

Genetic modification may be a more steady and reliable way to manipulate the character of DC. Generation of tolerogenic DC by forced expression of Fas ligand, indoleamine 2,3-dioxygemase, IL-10, or CTLA4Ig by gene transfer has been also reported (38–41). In a recent study, type II collagen-loaded bone marrow-derived DC genetically engineered to express TRAIL by using an adenovirus vector ameliorated type II collagen-induced arthritis (42).

Regarding methods for gene transfer to DC, electroporation, lipofection, and virus vector-mediated transfection have been reported (38–43). However, considering clinical applications, presently established methods have several drawbacks, i.e., efficiency of gene transfer, stability of gene expression, limitation of the size and number of genes to be introduced, potential risk accompanying the use of virus vectors, and the immunogenicity of the virus vectors. For the purpose of Ag-specific negative regulation of immune responses, the antigenicity of vector systems may lead to problems. Importantly, to efficiently down-modulate T cell responses in an Ag-specific manner, it is desirable to introduce multiple expression vectors to generate stable transfectant DC, which continuously present transgene-derived Ag and simultaneously express immunosuppressive molecules.

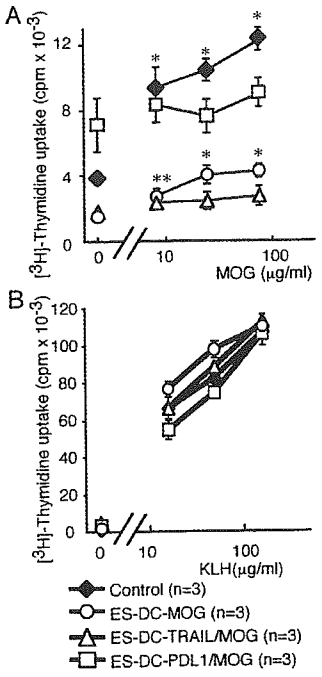

FIGURE 8. Inhibition of activation of MOG-reactive T cells and no effect of activation of KLH-specific T cell by treatment of mice with ES-DC expressing MOG plus TRAIL or PD-L1. *A*, Inguinal lymph node cells (3×10^5) were isolated from CBF_1 mice (three mice per group) of various treatment groups at over day 42, and were stimulated ex vivo with irradiated and MOG peptide-pulsed syngeneic spleen cells for 3 days. Proliferative response of T cells was quantified by [^{3}H]thymidine uptake in the last 12 h of the culture. The asterisks indicate that the differences in responses are statistically significant compared with count in the absence of Ag (*, $p < 0.01$; **, $p < 0.05$). The data are each representative of two independent and reproducible experiments with similar results. *B*, CBF_1 mice (three mice per group) were i.p. injected with ES-DC (1×10^6 cells/injection/mouse) on days −8, −5, and −2, and immunized with KLH/CFA on day 0. On day 11, inguinal lymph node cells were isolated and restimulated with the indicated concentration of KLH in vitro. Proliferation of T cells was quantified as described above.

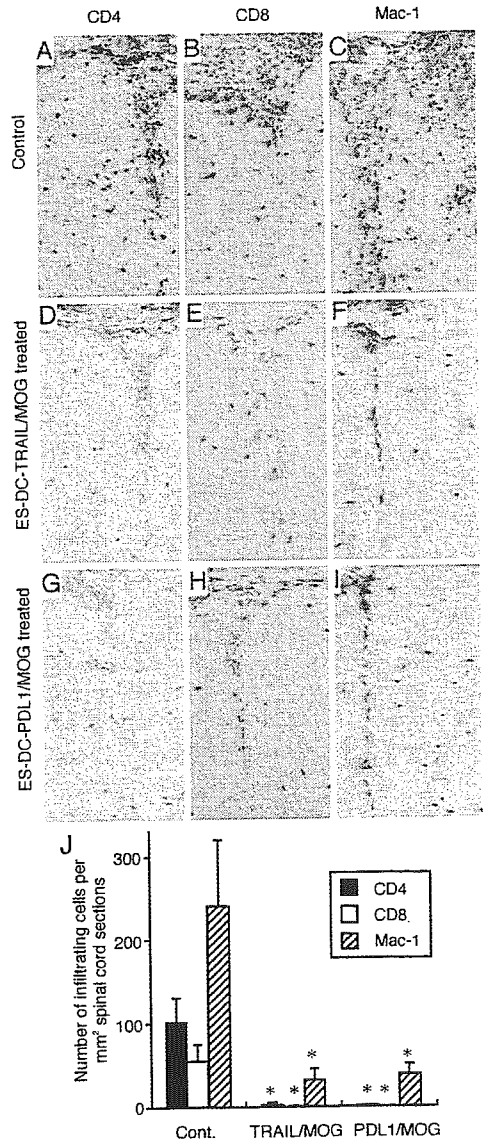

FIGURE 9. Inhibition of infiltration of $CD4^+$ T cells, $CD8^+$ T cells, and Mac-1^+ macrophages into spinal cord by treatment of mice with ES-DC expressing MOG plus TRAIL or PD-L1. Mice were pretreated with ES-DC-TRAIL/MOG, PDL1/MOG, or untreated and subsequently immunized according to the protocol for EAE induction as shown in Fig. 6*A*. The cervical, thoracic, and lumbar spinal cord was isolated at day 11 and subjected to immunohistochemical analysis. CD4 (*A*, *D*, and *G*), CD8 (*B*, *E*, and *H*), and Mac-1 (*C*, *F*, and *I*) staining are shown in representative untreated control (*A–C*), ES-DC-TRAIL/MOG-treated (*D–F*), and ES-DC-PDL1/MOG-treated (*G–I*) mice. *J*, The positive cells were microscopically counted in three sections of spinal cord. Results are expressed as mean ± SD of $CD4^+$, $CD8^+$, Mac-1^+ cells per 1 mm^2 tissue area of samples obtained from five mice. The asterisks indicate that the decreases in number of infiltrated cells are statistically significant ($p < 0.01$) compared with control.

Efficient genetic modification of mouse DC can be done by gene transfer to ES cells and subsequent differentiation of transfectant ES cells to ES-DC. By sequential transfection of ES cells using multiple expression vectors, transfectant ES-DC expressing multiple transgene products can readily be generated. In a recent study, we demonstrated that this methodology worked very effectively for induction of antitumor immunity, showing highly efficient stimulation of Ag-specific T cells by in vivo transfer of ES-DC expressing T cell-attracting chemokines along with Ag (20).

The present study demonstrates the usefulness of the genetically modified DC generated by this method for the treatment of subjects with autoimmune disease. We generated ES-DC presenting the MOG epitope in the context of MHC class II molecule and simultaneously expressing immunosuppressive molecule, TRAIL or PD-L1. By pre- or posttreatment of mice with such ES-DC, we succeeded in preventing an autoimmune disease model, EAE induced by immunization with MOG peptide (Figs. 6 and 7; Table II). Down-modulation of immune response by treatment with genetically modified ES-DC did not affect the immune response to irrelevant exogenous Ag, KLH (Fig. 8*B*). Thus, we achieved the prevention of EAE without decrease in the immune response to an irrelevant Ag.

As for the function of TRAIL, induction of apoptosis has been reported by several groups (3, 4, 42, 44). We also observed an increase in apoptosis of $CD4^+$ T cells in spleens of mice treated with ES-DC-TRAIL/MOG compared with ES-DC-MOG, PDL1/MOG or RPMI 1640 medium (control), as shown in Fig. 10. The result is consistent with a recent report by Liu et al. (42). They introduced the *TRAIL* gene into bone marrow-derived DC by adenovirus vector and injected the *TRAIL* transfectant DC into mice for prevention of collagen-induced arthritis, and also observed an increased number of apoptotic T cells in the injected mice. The

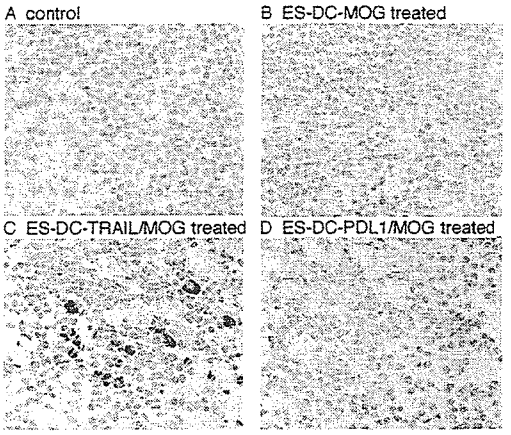

FIGURE 10. Induction of apoptosis of spleen cells by treatment of mice with ES-DC expressing TRAIL along with MOG peptide. Mice were treated with the indicated ES-DC and immunized with MOG peptide, following the schedule described in Fig. 6*A*. On day 11, spleens were isolated from the mice, and apoptotic cells were detected by in situ TUNEL staining. Original magnification, ×200. Sections of the mice untreated (*A*), treated with ES-DC-MOG (*B*), ES-DC-TRAIL/MOG (*C*), and ES-DC-PDL1/MOG (*D*) are shown. Similar results were observed for three mice used in each experimental group, and representative results are shown.

potential for ES-DC-TRAIL/MOG to cause apoptosis of T cells may have played some role in the protection from EAE, at least in part, in our experiments. In addition, our preliminary experiments suggest that ES-DC-TRAIL/MOG induced T cells with protective effects against EAE. In the experiments, we isolated splenic $CD4^+$ T cells from ES-DC-TRAIL/MOG-treated mice and adoptively transferred them to naive mice. The severity of subsequently induced EAE in the recipient mice was significantly reduced by this treatment (data not shown). At present, it may be possible that both induction of apoptosis of MOG-reactive pathogenic T cells and promotion of T cells with some regulatory function contributed to prevention of EAE by ES-DC-TRAIL/MOG. However, to clarify the precise mechanism or character of the T cell with regulatory function, further investigations are necessary.

In contrast, in case of treatment with ES-DC-PDL1/MOG, neither apoptosis of T cells nor induction of transferable disease-preventing T cells was observed (data not shown). We presume induction of anergy of MOG-reactive T cells to be likely as the mechanism of disease-preventive effect of treatment with ES-DC-PDL1/MOG, based on previous literature regarding the function of PD-L1 (7, 14, 45–47).

To determine whether the profile of cytokine production was altered by treatment with ES-DC, we did ELISA to quantify IL-10, IL-4, and IFN-γ produced by spleen cells of ES-DC-treated mice upon stimulation with MOG peptide in vitro. We observed no significant change in the amount of these cytokines produced by spleen cells from ES-DC-TRAIL/MOG-treated or ES-DC-PDL1/MOG-treated mice, compared with those from ES-DC-MOG-treated mice (data not shown). The level of expression of mRNA for TGF-β detected by RT-PCR was also unchanged compared with control (data not shown). Thus, involvement of IL-10-producing Tr-1 cells or Th2 cells in protection from EAE by treatment with ES-DC-TRAIL/MOG or ES-DC-PDL1/MOG is unlikely, although one cannot totally rule out the possibility.

The capacity of the ES cells to differentiate to ES-DC was never impaired even after culture for at least over 4 mo. Inactivation of transcription of introduced genes due to gene silencing in ES cells can be prevented using vectors bearing the IRES-drug resistance gene or by targeted gene introduction with an exchangeable gene-trap system (2). Thus, genetically manipulated ES cells can be used as an infinite source for DC with genetically modified properties.

Recently, we established methods for generation of DC from nonhuman primate ES cells and also for genetic modification of them (S. Senju, H. Suemori, H. Matsuyoshi, S. Hirata, Y. Uemura, Y.-Z. Chen, D. Fukuma, M. Furuya, N. Nakatsuji, and Y. Nishimura, manuscript in preparation). We hope to apply this method to human ES cells to generate genetically modified human ES-DC, although some modification might be necessary. In the future, Ag-specific immune modulation therapy by in vivo transfer of human ES-DC expressing antigenic protein along with immune-regulating molecules may well be realized, based on evidence in the current study in the mouse system. Possible applications of this technology are treatment of subjects with autoimmune and allergic diseases and also for induction of tolerance to transplanted organs, especially those generated from ES cells. Thus, the methods established in the present study may have implications as a broad medical technology.

Acknowledgments

We thank Dr. S. Aizawa (RIKEN Center for Developmental Biology, Kobe, Japan) for TT2, Drs. N. Takakura (Kanazawa University, Kanazawa, Japan) and T. Suda (Keio University, Tokyo, Japan) for OP9, Dr. H. Niwa (RIKEN Center for Developmental Biology, Kobe, Japan) for pCAG-IPuro, Drs. T. Okazaki and T. Honjo (Kyoto University, Kyoto, Japan) for a cDNA clone for PD-L1, Tatsuko Kubo (Department of Molecular Pathology, Kumamoto University) for technical assistance, and Kirin Brewery Co., Ltd., for rGM-CSF. M. Ohara (Fukuoka, Japan) provided helpful comments on the manuscript.

References

1. Fujii, S., S. Senju, Y. Z. Chen, M. Ando, S. Matsushita, and Y. Nishimura. 1998. The CLIP-substituted invariant chain efficiently targets an antigenic peptide to HLA class II pathway in L cells. *Hum. Immunol. 59:607.*
2. Senju, S., S. Hirata, H. Matsuyoshi, M. Masuda, Y. Uemura, K. Araki, K. Yamamura, and Y. Nishimura. 2003. Generation and genetic modification of dendritic cells derived from mouse embryonic stem cells. *Blood 101:3501.*
3. Wiley, S. R., K. Schooley, P. J. Smolak, W. S. Din, C. P. Huang, J. K. Nicholl, G. R. Sutherland, T. D. Smith, C. Rauch, C. A. Smith, and R. G. Goodwin. 1995. Identification and characterization of a new member of the TNF family that induces apoptosis. *Immunity 3:673.*
4. Kayagaki, N., N. Yamaguchi, M. Nakayama, K. Takeda, H. Akiba, H. Tsutsui, H. Okamura, K. Nakanishi, K. Okumura, and H. Yagita. 1999. Expression and function of TNF-related apoptosis-inducing ligand on murine activated NK cells. *J. Immunol. 163:1906.*
5. Lamhamedi-Cherradi, S. E., S. J. Zheng, K. A. Maguschak, J. Peschon, and Y. H. Chen. 2003. Defective thymocyte apoptosis and accelerated autoimmune diseases in $TRAIL^{-/-}$ mice. *Nat. Immunol. 4:255.*
6. Dong, H., G. Zhu, K. Tamada, and L. Chen. 1999. B7–H1, a third member of the B7 family, co-stimulates T-cell proliferation and interleukin-10 secretion. *Nat. Med. 5:1365.*
7. Freeman, G. J., A. J. Long, Y. Iwai, K. Bourque, T. Chernova, H. Nishimura, L. J. Fitz, N. Malenkovich, T. Okazaki, M. C. Byrne, et al. 2000. Engagement of the PD-1 immunoinhibitory receptor by a novel B7 family member leads to negative regulation of lymphocyte activation. *J. Exp. Med. 192:1027.*
8. Nishimura, H., M. Nose, H. Hiai, N. Minato, and T. Honjo. 1999. Development of lupus-like autoimmune diseases by disruption of the *PD-1* gene encoding an ITIM motif-carrying immunoreceptor. *Immunity 11:141.*
9. Nishimura, H., T. Okazaki, Y. Tanaka, K. Nakatani, M. Hara, A. Matsumori, S. Sasayama, A. Mizoguchi, H. Hiai, N. Minato, and T. Honjo. 2001. Autoimmune dilated cardiomyopathy in PD-1 receptor-deficient mice. *Science 291:319.*
10. Song, K., Y. Chen, R. Goke, A. Wilmen, C. Seidel, A. Goke, and B. Hilliard. 2000. Tumor necrosis factor-related apoptosis-inducing ligand (TRAIL) is an inhibitor of autoimmune inflammation and cell cycle progression. *J. Exp. Med. 191:1095.*
11. Hilliard, B., A. Wilmen, C. Seidel, T. S. Liu, R. Goke, and Y. Chen. 2001. Roles of TNF-related apoptosis-inducing ligand in experimental autoimmune encephalomyelitis. *J. Immunol. 166:1314.*
12. Lunemann, J. D., S. Waiczies, S. Ehrlich, U. Wendling, B. Seeger, T. Kamradt, and F. Zipp. 2002. Death ligand TRAIL induces no apoptosis but inhibits activation of human (auto)antigen-specific T cells. *J. Immunol. 168:4881.*
13. Kayagaki, N., N. Yamaguchi, M. Abe, S. Hirose, T. Shirai, K. Okumura, and H. Yagita. 2002. Suppression of antibody production by TNF-related apoptosis-inducing ligand (TRAIL). *Cell. Immunol. 219:82.*

14. Nishimura, H., and T. Honjo. 2001. PD-1: an inhibitory immunoreceptor involved in peripheral tolerance. *Trends Immunol. 22:265.*
15. Okazaki, T., Y. Iwai, and T. Honjo. 2002. New regulatory co-receptors: inducible co-stimulator and PD-1. *Curr. Opin. Immunol. 14:779.*
16. Salama, A. D., T. Chitnis, J. Imitola, M. J. Ansari, H. Akiba, F. Tushima, M. Azuma, H. Yagita, M. H. Sayegh, and S. J. Khoury. 2003. Critical role of the programmed death-1 (PD-1) pathway in regulation of experimental autoimmune encephalomyelitis. *J. Exp. Med. 198:71.*
17. Liang, S. C., Y. E. Latchman, J. E. Buhlmann, M. F. Tomczak, B. H. Horwitz, G. J. Freeman, and A. H. Sharpe. 2003. Regulation of PD-1, PD-L1, and PD-L2 expression during normal and autoimmune responses. *Eur. J. Immunol. 33:2706.*
18. Ansari, M. J., A. D. Salama, T. Chitnis, R. N. Smith, H. Yagita, H. Akiba, T. Yamazaki, M. Azuma, H. Iwai, S. J. Khoury, et al. 2003. The programmed death-1 (PD-1) pathway regulates autoimmune diabetes in nonobese diabetic (NOD) mice. *J. Exp. Med. 198:63.*
19. Fairchild, P. J., F. A. Brook, R. L. Gardner, L. Graca, V. Strong, Y. Tone, M. Tone, K. F. Nolan, and H. Waldmann. 2000. Directed differentiation of dendritic cells from mouse embryonic stem cells. *Curr. Biol. 10:1515.*
20. Matsuyoshi, H., S. Senju, S. Hirata, Y. Yoshitake, Y. Uemura, and Y. Nishimura. 2004. Enhanced priming of antigen-specific CTLs in vivo by embryonic stem cell-derived dendritic cells expressing chemokine along with antigenic protein: application to antitumor vaccination. *J. Immunol. 172:776.*
21. Fairchild, P. J., K. F. Nolan, S. Cartland, L. Graca, and H. Waldmann. 2003. Stable lines of genetically modified dendritic cells from mouse embryonic stem cells. *Transplantation 76:606.*
22. Cheng, P., Y. Nefedova, L. Miele, B. A. Osborne, and D. Gabrilovich. 2003. Notch signaling is necessary but not sufficient for differentiation of dendritic cells. *Blood 102:3980.*
23. Mendel, I., N. Kerlero de Rosbo, and A. Ben-Nun. 1995. A myelin oligodendrocyte glycoprotein peptide induces typical chronic experimental autoimmune encephalomyelitis in H-2^b mice: fine specificity and T cell receptor Vβ expression of encephalitogenic T cells. *Eur. J. Immunol. 25:1951.*
24. Greer, J. M., R. A. Sobel, A. Sette, S. Southwood, M. B. Lees, and V. K. Kuchroo. 1996. Immunogenic and encephalitogenic epitope clusters of myelin proteolipid protein. *J. Immunol. 156:371.*
25. Zamvil, S. S., D. J. Mitchell, M. B. Powell, K. Sakai, J. B. Rothbard, and L. Steinman. 1988. Multiple discrete encephalitogenic epitopes of the autoantigen myelin basic protein include a determinant for I-E class II-restricted T cells. *J. Exp. Med. 168:1181.*
26. Senju, S., K. Iyama, H. Kudo, S. Aizawa, and Y. Nishimura. 2000. Immunocytochemical analyses and targeted gene disruption of GTPBP1. *Mol. Cell. Biol. 20:6195.*
27. Fujii, S., Y. Uemura, L. K. Iwai, M. Ando, S. Senju, and Y. Nishimura. 2001. Establishment of an expression cloning system for $CD4^+$ T cell epitopes. *Biochem. Biophys. Res. Commun. 284:1140.*
28. Uemura, Y., S. Senju, K. Maenaka, L. K. Iwai, S. Fujii, H. Tabata, H. Tsukamoto, S. Hirata, Y. Z. Chen, and Y. Nishimura. 2003. Systematic analysis of the combinatorial nature of epitopes recognized by TCR leads to identification of mimicry epitopes for glutamic acid decarboxylase 65-specific TCRs. *J. Immunol. 170:947.*
29. Weir, C. R., K. Nicolson, and B. T. Backstrom. 2002. Experimental autoimmune encephalomyelitis induction in naive mice by dendritic cells presenting a self-peptide. *Immunol. Cell Biol. 80:14.*
30. Legge, K. L., R. K. Gregg, R. Maldonado-Lopez, L. Li, J. C. Caprio, M. Moser, and H. Zaghouani. 2002. On the role of dendritic cells in peripheral T cell tolerance and modulation of autoimmunity. *J. Exp. Med. 196:217.*
31. Bonham, C. A., L. Lu, R. A. Banas, P. Fontes, A. S. Rao, T. E. Starzl, A. Zeevi, and A. W. Thomson. 1996. TGF-β1 pretreatment impairs the allostimulatory function of human bone marrow-derived antigen-presenting cells for both naive and primed T cells. *Transpl. Immunol. 4:186.*
32. Lutz, M. B., R. M. Suri, M. Niimi, A. L. Ogilvie, N. A. Kukutsch, S. Rossner, G. Schuler, and J. M. Austyn. 2000. Immature dendritic cells generated with low doses of GM-CSF in the absence of IL-4 are maturation resistant and prolong allograft survival in vivo. *Eur. J. Immunol. 30:1813.*
33. Steinbrink, K., M. Wolfl, H. Jonuleit, J. Knop, and A. H. Enk. 1997. Induction of tolerance by IL-10-treated dendritic cells. *J. Immunol. 159:4772.*
34. Menges, M., S. Rossner, C. Voigtlander, H. Schindler, N. A. Kukutsch, C. Bogdan, K. Erb, G. Schuler, and M. B. Lutz. 2002. Repetitive injections of dendritic cells matured with tumor necrosis factor-α induce antigen-specific protection of mice from autoimmunity. *J. Exp. Med. 195:15.*
35. Sato, K., N. Yamashita, M. Baba, and T. Matsuyama. 2003. Regulatory dendritic cells protect mice from murine acute graft-versus-host disease and leukemia relapse. *Immunity 18:367.*
36. Sato, K., N. Yamashita, M. Baba, and T. Matsuyama. 2003. Modified myeloid dendritic cells act as regulatory dendritic cells to induce anergic and regulatory T cells. *Blood 101:3581.*
37. Dhodapkar, M. V., R. M. Steinman, J. Krasovsky, C. Munz, and N. Bhardwaj. 2001. Antigen-specific inhibition of effector T cell function in humans after injection of immature dendritic cells. *J. Exp. Med. 193:233.*
38. Takayama, T., Y. Nishioka, L. Lu, M. T. Lotze, H. Tahara, and A. W. Thomson. 1998. Retroviral delivery of viral interleukin-10 into myeloid dendritic cells markedly inhibits their allostimulatory activity and promotes the induction of T-cell hyporesponsiveness. *Transplantation 66:1567.*
39. Lu, L., A. Gambotto, W. C. Lee, S. Qian, C. A. Bonham, P. D. Robbins, and A. W. Thomson. 1999. Adenoviral delivery of CTLA4Ig into myeloid dendritic cells promotes their in vitro tolerogenicity and survival in allogeneic recipients. *Gene Ther. 6:554.*
40. Min, W. P., R. Gorczynski, X. Y. Huang, M. Kushida, P. Kim, M. Obataki, J. Lei, R. M. Suri, and M. S. Cattral. 2000. Dendritic cells genetically engineered to express Fas ligand induce donor-specific hyporesponsiveness and prolong allograft survival. *J. Immunol. 164:161.*
41. Terness, P., T. M. Bauer, L. Rose, C. Dufter, A. Watzlik, H. Simon, and G. Opelz. 2002. Inhibition of allogeneic T cell proliferation by indoleamine 2,3-dioxygenase-expressing dendritic cells: mediation of suppression by tryptophan metabolites. *J. Exp. Med. 196:447.*
42. Liu, Z., X. Xu, H. C. Hsu, A. Tousson, P. A. Yang, Q. Wu, C. Liu, S. Yu, H. G. Zhang, and J. D. Mountz. 2003. CII-DC-AdTRAIL cell gene therapy inhibits infiltration of CII-reactive T cells and CII-induced arthritis. *J. Clin. Invest. 112:1332.*
43. Morita, Y., J. Yang, R. Gupta, K. Shimizu, E. A. Shelden, J. Endres, J. J. Mule, K. T. McDonagh, and D. A. Fox. 2001. Dendritic cells genetically engineered to express IL-4 inhibit murine collagen-induced arthritis. *J. Clin. Invest. 107:1275.*
44. Giovarelli, M., P. Musiani, G. Garotta, R. Ebner, E. Di Carlo, Y. Kim, P. Cappello, L. Rigamonti, P. Bernabei, F. Novelli, et al. 1999. A "stealth effect": adenocarcinoma cells engineered to express TRAIL elude tumor-specific and allogeneic T cell reactions. *J. Immunol. 163:4886.*
45. Brown, J. A., D. M. Dorfman, F. R. Ma, E. L. Sullivan, O. Munoz, C. R. Wood, E. A. Greenfield, and G. J. Freeman. 2003. Blockade of programmed death-1 ligands on dendritic cells enhances T cell activation and cytokine production. *J. Immunol. 170:1257.*
46. Carter, L., L. A. Fouser, J. Jussif, L. Fitz, B. Deng, C. R. Wood, M. Collins, T. Honjo, G. J. Freeman, and B. M. Carreno. 2002. PD-1:PD-L inhibitory pathway affects both $CD4^+$ and $CD8^+$ T cells and is overcome by IL-2. *Eur. J. Immunol. 32:634.*
47. Selenko-Gebauer, N., O. Majdic, A. Szekeres, G. Hofler, E. Guthann, U. Korthauer, G. Zlabinger, P. Steinberger, W. F. Pickl, H. Stockinger, et al. 2003. B7–H1 (programmed death-1 ligand) on dendritic cells is involved in the induction and maintenance of T cell anergy. *J. Immunol. 170:3637.*

Parasitology Research
© Springer-Verlag 2005
DOI 10.1007/s00436-004-1296-0

Original Paper

Expression of TGF-β-like molecules in the life cycle of *Schistosoma japonicum*

M. Hirata (✉) · K. Hirata · T. Hara · M. Kawabuchi · T. Fukuma

M. Hirata · T. Hara · T. Fukuma
Department of Parasitology, Kurume University School of Medicine, 830-0011 Kurume, Japan

K. Hirata · M. Kawabuchi
Department of Anatomy and Cell Biology, Graduate School of Medical Sciences, Kyushu University, 812-8582 Fukuoka , Japan

✉ M. Hirata
Phone: +81-942-317550
Fax: +81-942-310344
E-mail: hiramizu@med.kurume-u.ac.jp

Received: 19 November 2004 / **Accepted:** 23 November 2004

Abstract The transforming growth factor β (TGF-β) family controls an extremely wide range of biological activities, such as the growth and differentiation of cells, and immunological events against infectious agents. Although TGF-β homologs appear to be widely present in metazoan animals, studies of parasite-derived molecules are relatively few. Using antibodies against anti-mouse TGF-β_1, -β_2, and -β_3, we show the expression of TGF-β-like molecules in *Schistosoma japonicum* cercariae, schistosomula, eggs and adult worms. Intense immunoreactivity was found on the surface of free-living cercarial bodies. In transverse sections of cercariae, the molecules were localized in the tegument and subtegumental cells, and the number and distribution of producing cells significantly differed with each antibody. In the skin-migrating stage, the expression in the tegumental surface gradually decreased and became almost negative within 48 h of exposure. In adult worms and eggs, the reactivity was found in subtegumental cells and in cells of a tubular structure, respectively. In western blot analysis, the detection of conventional TGF-β molecules failed. The expression of TGF-b-like molecules was distinctly regulated at each developmental stage.

Introduction

Transforming growth factor-β (TGF-β) is produced by a variety of mammalian host cells and plays a diversity of roles. The TGF-β family is essential for the growth and differentiation of cells and for morphogenesis (Kingsley 1994), and TGF-β is also an important modulator of immune cell activities, together with IL-4 and IL-10 (Letterio and Roberts 1998; Cobbold and Waldmann 1998). Induction and production of TGF-β during microbe infection has been reported to seriously affect the outcome of the disease (reviewed by Omer et al. 2000). In *Schistosoma mansoni* infection, TGF-β has been reported to be significantly involved in the regulation of macrophage cytotoxic activity (Oswald et al. 1992; Williams et al. 1995), or in the granulomatous response against eggs (Wahl et al. 1997; Mola et al. 1999).

The TGF-β family, related homologs and their corresponding receptors appear to be anciently conserved from nematodes to mammals. *Caenorhabditis elegans*, a well-studied free-living soil nematode, utilizes the TGF-β signaling system in dauer formation (Riddle and Albert 1997). The presence of two TGF-β homologs has been reported in parasitic nematodes: *tgh-1* in *Brugia malayi* and *B. pahangi* (Gomez-Escobar et al. 1998), and *tgh-2* in *B. malayi* (Gomez-Escobar et al. 2000). The type I TGF-β receptor, Bp-trk-1, has been isolated from the *Brugia* species (Gomez-Escobar et al. 1997). In *S. mansoni*, SmRK1, a member of TGF-β receptor family, is expressed on the surface of male worms (Davies et al. 1998; Beall et al. 2000) and host-derived TGF-β is a ligand of SmRK1 (Beall and Pearce 2001).

Schistosoma japonicum parasites are multicellular eukaryotic organisms that have a complex life cycle and are prevalent in South-east Asia. Schistosome worms settle in the portal vein and the eggs, which are continuously laid, cause severe intestinal and hepatosplenic disease. Here, we report that TGF-β immunoreactive molecules are expressed during the whole life cycle of *S. japonicum* (eggs, cercariae, schistosomula and adult worms), and that they are distinctly regulated at each developmental stage.

Materials and methods

Animals, parasites and preparation of materials

The Japanese strain of *S. japonicum* has been maintained in our laboratory for 25 years by passage through *Oncomelania hupensis nosophora* and rabbits. C57BL/6 female mice were purchased from the Shizuoka Laboratory Animal Center (SLC), Japan.

Fresh cercariae emerging from infected snails were fixed in 4% paraformaldehyde in 0.13 M phosphate buffer. Some were processed for whole mount preparations; they were placed on slides coated with poly-L-lysine and fixed again in paraformaldehyde. The other fixed cercariae were implanted into mouse livers through the cecal vein to investigate the details of the TGF-beta-immunoreactive structure. The liver was removed and fixed in the same fixative 30 min later. To investigate the skin migrating stage of schistosomula, mice were percutaneously exposed to 100 cercariae on the shaved abdomen by the ring method. Mice were killed 0.5, 8, 24, and 48 h later. The exposed site was removed and fixed in the paraformaldehyde solution. Livers containing deposited eggs and adult worms were collected from mice infected for 7 weeks and fixed with the same fixative. Paraformaldehyde fixed specimens were routinely processed and embedded in paraffin wax, and sections (4–10 μm thickness) were cut.

For western blot analysis, cercariae were pelleted by centrifugation, sonicated and ground using polytron (Kinematica, Switzerland). The preparation of egg and adult worm extracts was described previously (Hirata et al. 1997). To collect eggs, infected mouse livers and intestines were digested with pronase and collagenase and filtered through several meshes. Eggs were washed with phosphate-buffered saline (PBS) six times by light centrifugation (600 rpm, 2 min).

Immunohistochemistry

For immunoenzyme staining, the sections and whole-mount preparations were preincubated with Block Ace (Yukijirushi, Japan) for 1 h at room temperature (RT) followed by either rabbit anti-mouse TGF-β_1, -β_2 or -β_3 antibody (raised against C-terminal peptide, Santa Cruz, Santa Cruz, Calif)(1:100) or normal rabbit IgG, as a control, overnight. They were incubated with biotinylated anti-rabbit IgG (1:200) (Vector Laboratories, Burlingame, Calif.) for 1 h and endogenous peroxidase activity was blocked with methanol containing 10% H_2O_2. After incubation with the avidin-biotin-peroxidase complex (Vector) for 50 min, reactions were developed with 3-amino-9-ethylcarbazole. The slides were counterstained with Meyer's hematoxylin.

The fluorescent immunohistochemical procedure was as described previously (Hirata et al. 2000, 2003). Briefly, the sections and whole-mount preparations were incubated with antibody to TGF-β_1, -β_2 or -β_3 diluted 1:100 in PBS overnight at RT, and then with FITC-conjugated horse anti-rabbit IgG (Vector) for 4 h at RT. To identify the cell nuclei, the sections and whole-mount preparations were counterstained with propidium iodide (PI) by using Vectashield mounting medium with PI (Vector).

Controls were processed identically and in parallel, however, they were incubated with non-immune rabbit IgG (1:100) rather than with primary antibodies. In the peptide blocking test, primary antibodies were mixed with each corresponding blocking peptide of TGF-β_1, -β_2 or -β_3 (Santa Cruz) at a 1:2 or 1:4 molar ratio and incubated overnight at 4°C and staining was performed as above. In some experiments, antibodies were mixed with an unrelated peptide (anti-TGF-β_3 plus TGF-β_1 blocking peptide) to confirm the specificity.

Confocal laser scanning microscopy

The sections and whole mount preparations double-labeled with FITC and PI were scanned using excitation at 488 nm (argon laser) for FITC and at 568 nm (krypton laser) for PI with a confocal laser scanning imaging system (LSM-GB200 or LSM-FV300, Olympus, Japan). Optical sections of the Z-series of each fluorescence (at consecutive focal levels of 1 μm) were separately taken on channel 1 and channel 2 to avoid any cross-talk and then superimposed. For whole-mount cercariae, the images of both fluorescences were further overlaid with differential interference contrast (DIC) images by LSM-FV300. For analyzing the entire features of cercariae, the images of the Z-series were examined side by side and added to reconstruct a single two-dimensional image. The images were taken using a 10×, 20× or 40× objective lens.

Western blot analysis

The protein concentration of schistosome extracts was determined by Micro BCA protein assay (Pierce, Rockford, Ill.). The extracts were dissolved in reducing sample buffer containing 50 mM Tris-HCl (pH 6.8), 2% SDS, 0.6% 2-mercaptoethanol, 10% glycerin and 0.03% bromophenol blue, and analyzed using 12.5% polyacrylamide gels in the presence of SDS (Laemmli 1970). Proteins were transferred onto PVDF membrane. The membrane was blocked with 100% Block Ace at 4°C for 16 h and then immunoenzymatically labeled using anti-TGF-β_1, -β_2 or -β_3 antibody (1:1000) and peroxidase-conjugated goat anti-rabbit IgG (1:10,000) (Vector). The reaction was developed by SuperSignal West Pico Chemiluminescent substrate (Pierce).

4

Results

Immunoreactivity in skin stage

Immunoenzyme staining of cercariae-exposed mouse skin (0.5 h) revealed immunoreactivity for all TGF-β isoforms, TGF-β_1, -β_2 and -β_3, in the body of schistosomula, i.e. at the surface and inside the body (Fig. 1a–c). In control studies, no specific reactivity was seen when the primary antibody was substituted with normal rabbit IgG. In the peptide blocking study, no reactivity was seen (a representative experiment is shown in Fig. 1d), and parallel control experiments that used unrelated peptides did not affect the reactivity. Thus, the expression of TGF-β-like molecules in parasites was considered to be specific. Similar experiments were performed on the fluorescence-labeled specimens (below) and confirmed the specificity.

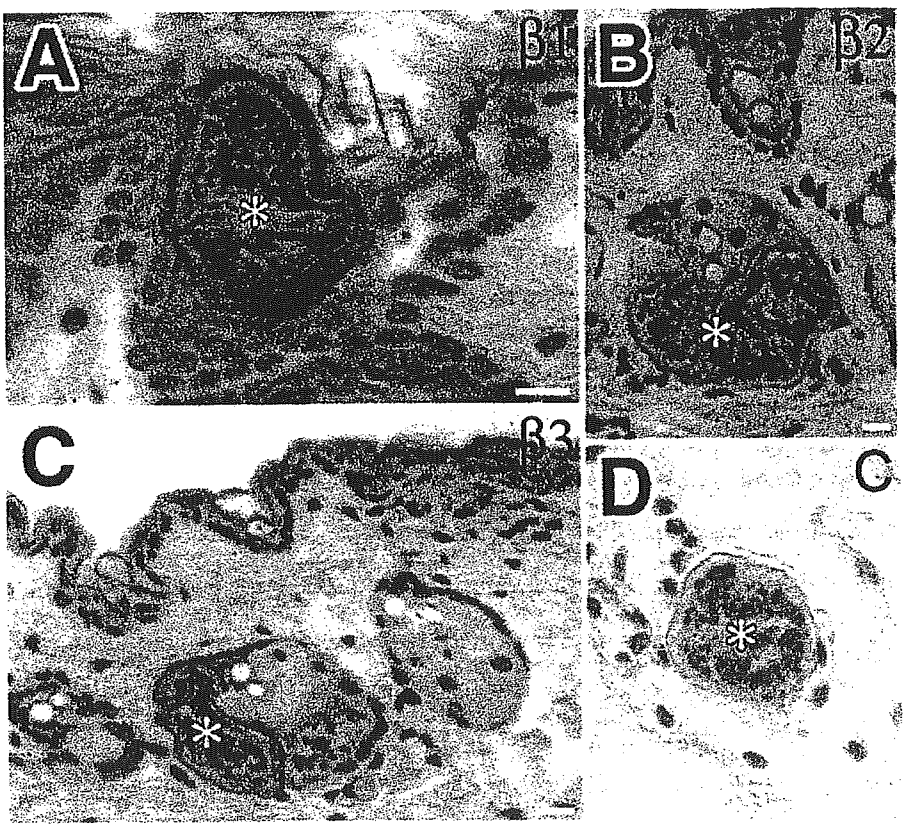

Fig. 1 Expression of TGF-β isoforms in 0.5-h schistosomula of *Schistosoma japonicum*. **a** Immunoenzyme staining of TGF-β_1, **b** TGF-β_2, and **C** TGF-β_3 is shown. Strong immunoreactivity for each TGF-β isoform was localized at the surface of schistosomulum (*asterisks*). Note that weak immunoreactivity for TGF-β_2 (**b**) and TGF-β_3 (**c**) was seen in the epidermis of mouse skin. **d** In a blocking test for TGF-β_3, no immunoreactivity was evident at the surface of schistosomula (*asterisk*). *Bar* 10 μm

5

Localization of TGF-β isoforms in cercariae

We investigated the detailed localization of each immunoreactive TGF-β isoform using cercariae that were previously paraformaldehyde-fixed and implanted into the mouse liver. Confocal laser scanning microscopy (CLSM) showed specific localization of all TGF-β isoforms in the tegument and the presence of cells expressing TGF-β-like molecules in the subtegumental area (Fig. 2a–c). The number and distribution of producing cells or cellular localization of immunoreactive molecules differed significantly with each isoform. For TGF-β_1, only a few immunoreactive cells were found in the subtegumental area (Fig. 2A), and its expression appeared to be limited to only a part of the cytoplasm, while the parasite tegument was intensely stained. Another characteristic finding for TGF-β_1 was strong reactivity at one region of the parasite surface. The Z-series of CLSM images on the whole parasite body revealed that this region had a pot-like structure (Fig. 2d). Comparison with serial sections, hematoxylin-eosin (H-E) stained preparations and with the previously described diagram of cercariae (Takahashi 1928), showed this region to be the ventral sucker.

TGF-β_2-immunoreactive elements were distributed diffusely over the body (Fig. 2b). In addition, the immunoreactivity at the tegument was rather weak compared with that for TGF-β_1 or TGF-β_3. TGF-β_3-immunoreactive cells were more numerous and stronger in intensity at the subtegumental area in comparison with TGF-β_1 and TGF-β_2 (Fig. 2c). Furthermore, in some TGF-β_3-immunoreactive cells, cytoplasmic processes (arrows) appeared to be continuous with the tegument, suggesting the molecules were being carried to the surface. In order to determine whether TGF-β-like molecules are mouse host-driven or not, whole mount preparations of free-living cercariae were analyzed by both CLSM and DIC after fluorescent immunohistochemical staining. The immunoreactivity was consistently recognized on the whole surface of the cercarial body, suggesting that the molecules are not derived from mouse host (Fig. 2e).

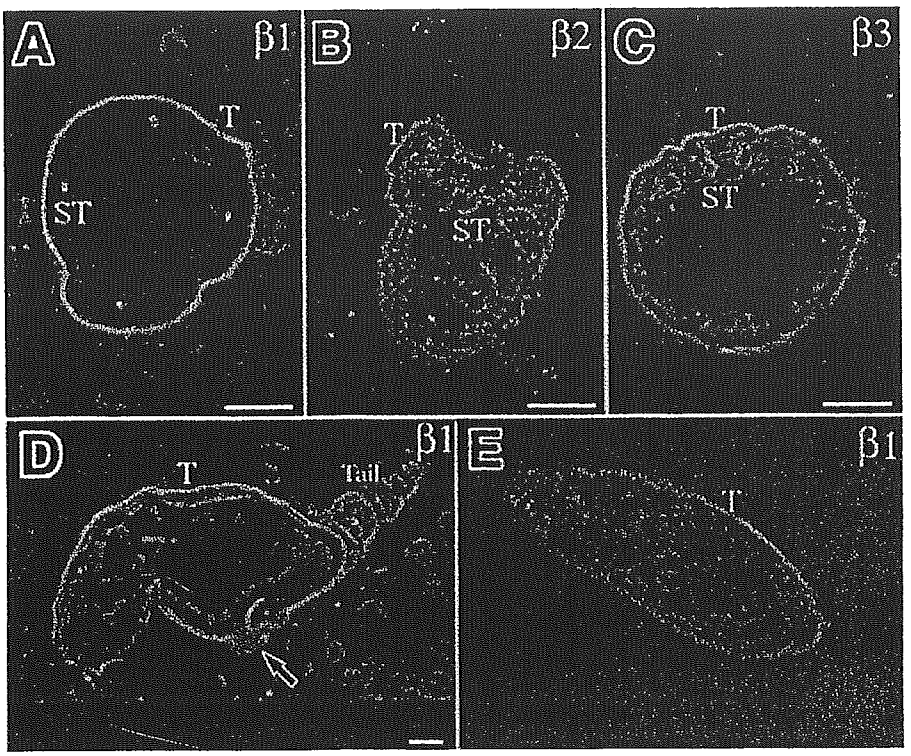

delete

Fig. 2 Detail of the localization of TGF-β isoforms in *S. japonicum* cercariae, which were embedded into the mouse liver (**a–d**) and was prepared in free-living condition (**e**). **a–c** Distribution of TGF-β_1, β_2 and β_3, respectively, in transverse sections of cercaria. ~~*Arrows* in **c** show cytoplasmic processes.~~ **d** TGF-β_1 in a longitudinally-sectioned cercaria. Three images of the Z-series with a distance of 3 μm were overlaid. Note the intensely stained pot-like structure (*arrow* in **d**), which was regarded as the ventral sucker. *Bar* 10 μm. **e** Localization of TGF-β_1 in the surface of a cercaria in a whole-mount preparation. Fluorescent immunoreactivity for TGF-β_1 is shown as *green* (FITC), whereas nuclei are *red* (PI). *Bar* 50 μm. *T* Tegument, *ST* subtegumental cell

Changes in immunoreactivity in the skin migrating stage

When TGF-β expression was examined at 8, 24 and 48 h after cercarial exposure to the skin, immunohistochemical findings for all isoforms in 8-h schistosomula were similar to those seen in cercariae prior to exposure (see Fig. 2) and 0.5-h schistosomula (see Fig. 1) in intensity and distribution (representative results for TGF-β_1 are shown in Fig. 3a). For 24 h schistosomula that migrated to the deeper part of the skin, less immunoreactivity in the tegument was found (data not shown). In 48-h schistosomula (Fig. 3b–d), the immunoreactivity in the tegument became almost negative or very faint at the surface. Thus, the expression of TGF-β-like molecules significantly decreased during the skin migrating stage.

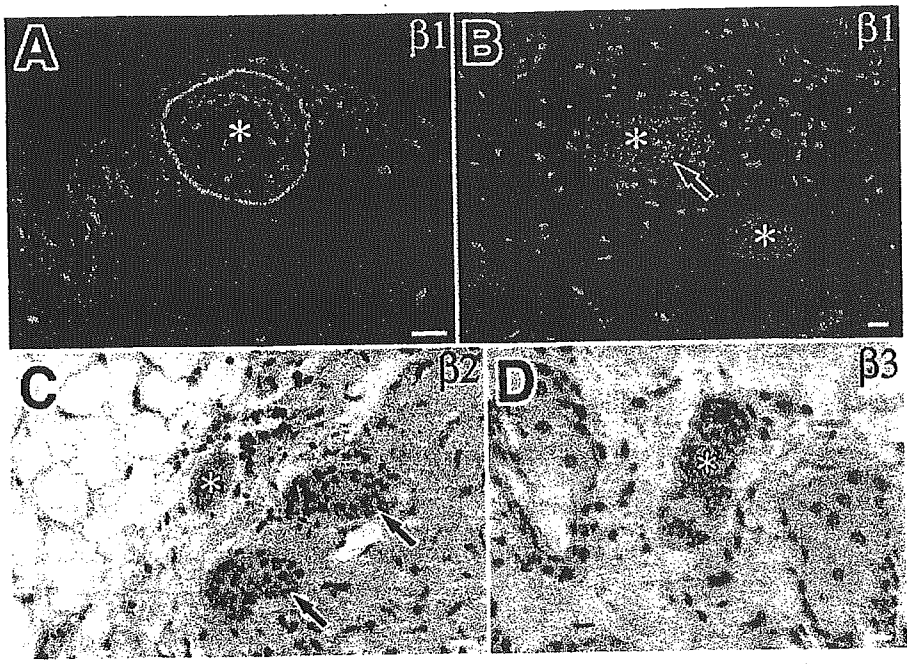

Fig. 3 Changes in TGF-β expression during the skin migrating stage of *S. japonicum* schistosomula. Expression of TGF-β in 8-h (**a**) and 48-h (**b–d**) schistosomula is shown. **a, b** Immunofluorescent staining; **c, d** immunoenzyme staining. At 8 h the expression of TGF-β_1 in the tegument was still strong (**a**), but had become faint at 48 h (**b**). Expression of TGF-β_2 (**c**) and TGF-β_3 (**d**) took a similar course and disappeared at 48 h. *Asterisks* indicate schistosomula. Note that strong immunoreactivity of TGF-β_1 in the presumed ventral sucker (*arrow* in **b**) remained at 48 h. Weak immunoreactivity for TGF-β_2 was seen in the appendages of the mouse skin (*arrows* in **c**). *Bar* 10 μm

Immunoreactivity in adult worms and eggs

In adult worms, TGF-β_3 immunoreactivity was apparent in subtegumental cells and the lining of gut epithelial cells of males and females (Fig. 4a). Following the peptide blocking test (Fig. 4b), fluorescence completely diminished in the subtegumental cells, but remained in the lining of gut epithelial cells, indicating that only the subtegumental cells were specifically stained. Although other TGF-β isoforms were examined, consistent results were only obtained in TGF-β_3.

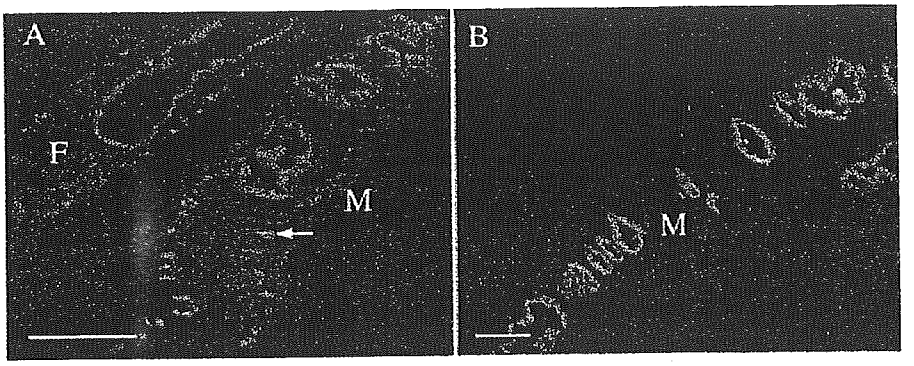

Fig. 4 Immunoreactivity of TGF-β_3 in adult worms. Prior to staining, the primary antibody was incubated with: **a** phosphate-buffered saline or **b** with the corresponding blocking peptide. Subtegumental cells (**a**, *arrow*) were considered as specific, since the reactivity disappeared in the blocking test (**b**). Homogeneous fluorescence in the gut epithelium was unchanged (**b**). *M* Male, *F* female. *Bar* 100 μm

Eggs deposited in the liver also showed strong immunoreactivity for TGF-β_2 on epithelial cells of a tubular-like structure of the miracidial larva (Fig. 5). The positively-stained tissue appeared to be a penetration gland and the associated duct. Other TGF-β isoforms did not yield any consistent results.

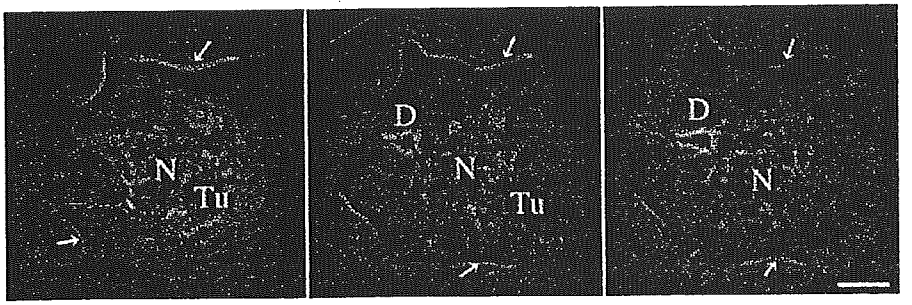

Fig. 5 Localization of TGF-β_1 in a *S. japonicum* egg deposited in mouse liver. Three images of the Z-series reveal TGF-β_2 immunoreactivity in cells of a tubular structure (*Tu*), which was regarded as one of the penetration glands, as well as in the associated duct (*D*). The neural mass (*N*) at the center was considered as negative. *Arrows* indicate eggshell. *Bar* 10 μm

Western blot analysis

In the western blot analysis of cercaria, egg and adult worm extracts, anti-TGF-β antibodies reacted with some molecules under reducing conditions, but differed from the consensus on the mature size of TGF-β (12.5 kDa) (data not shown), suggesting that the immunoreactive molecules found

in this study differ from generally-recognized TGF-β subfamily members with regard to molecular size.

Discussion

We report for the first time the presence of TGF-β-like-immunoreactive molecules throughout the *S. japonicum* life cycle (eggs, cercariae, schistosomula and adult worms). The most prominent expression of TGF-β-like molecules was detected in the tegument covering the whole body of cercariae at the larval stage. CLSM revealed that the molecules may possibly be produced in subtegumental cells and carried to the tegument, as was more evident for TGF-β_3 than the two other isoforms. Consistent expression in the tegument of the body and even the tail seems to reflect a flowing of the surface structure. In addition, the expression in cercariae prior to their penetration into the skin excluded the possibility that the molecules are derived from the mouse host. The specificity of each immunoreactive molecule was confirmed in several control experiments. In particular, our finding that inhibition was observed with the use of each corresponding blocking peptide, but not with unrelated peptides, strongly indicated specificity. In western blot analyses of egg, cercaria and adult worm extract, no band of the expected size was detected, and thus there is some difficulty in identifying the molecular basis of the immunoreactive molecules detected. Nevertheless, our study provides substantial evidence that TGF-β-like molecules that share cross-reactive epitopes with vertebrate TGF-βs are present in the parasites.

TGF-β-like molecules were expressed during the whole life cycle of the parasite, and significant differences were found in the distribution, producing cells and extent of expression with each isoform. In cercariae, TGF-β_2-, and -β_3-immunoreactive cells were greater in number and more widely distributed over the parasite body, whereas TGF-β_1-immunoreactive cells were very few and only a part of the cell body showed reactivity (Fig. 2A). TGF-β_3 and $-\beta_2$ were the predominant isoforms in adult worms and eggs, respectively, although the expression of other isoforms cannot be excluded. These different expression patterns invoke distinct roles for these isoforms during development.

Free-swimming cercariae markedly change their structure and their metabolic activity during transformation from cercaria to schistosomulum to protect themselves against osmotic changes and immune attack from host factors. Studies have shown that within 3 h of skin penetration, the glycocalyx coating of cercaria surface disappears and the trilaminate structure of cercariae, supplied from membranous elements of the subtegumental cells, changes to hepta- or more multi-laminate

and is continuously renewed, which is known to be an essential process for the development of the parasite (Hockley 1973; Sobhon and Upatham 1990). The TGF-β-like molecules identified in our study were localized in the tegument and appeared to be supplied from underlying cells, suggesting that the molecules appear to be one of the tegumental constituents. They continued to be expressed in 8-h schistosomula and then gradually decreased and became almost negative 48 h after skin penetration. This process differed temporally from the dynamic process of the tegumental structure or glycocalyx. Thus, the expression of these molecules appeared to be regulated differently from that of known surface structures. In contrast to the situation in cercariae or schistosomula, the reactive molecules in adult worms were not found in the tegument and there were no indications of transfer from subtegumental cells. In eggs, the molecules were expressed in cells of a tubular structure, suggesting that the molecule is secretory in nature. On the whole, the immunoreactive molecules appear to be involved in distinct roles at each developmental stage.

Here we have shown substantial evidence of TGF-β-immunoreactive molecule expression in most stages of *S. japonicum*, and their stage-specificity suggests a close association with their developmental process. In other studies on parasites, the existence of host cytokine-like molecules, such as homologs of migration inhibition factor in *Burgia malayi* (Pastrana et al. 1998; Pennock et al. 1998), IFN-γ-like protein in *Trichuris muris* (Grencis and Entwistle 1997) and IL-4-like molecules in *Anisakis simplex* (Cuellar et al. 2001) have been reported. In western blot analysis, however, we could not find generally recognized sizes of molecules. In addition, recent analysis of transcriptomes in *S. japonicum* (Hu et al. 2003) and *S. mansoni* (Verjovski-Almeida et al. 2003) has failed to detect conventional TGF-β molecules, suggesting that the molecules differ from conventional ones at least. In another set of experiments which examined TGF-β-like function in schistosome extracts using the Mv1Lu cell proliferation inhibition assay, we found strong inhibitory activity in soluble egg extract and moderate inhibition in worm extract. However, possible contamination of host derived substances or of protease activity in the extracts could not be excluded in the study. Further intensive studies are required to identify the genetic loci and clarify how the TGF-β-like molecules are involved in parasite development.

Acknowledgements The authors thank Ms. Manami Ohba (Department of Parasitology, Kurume University) for her excellent technical assistance. We also express thanks to Mr. Takaaki Kanemaru (Morphology Core, Graduate School of Medical Science, Kyushu University) for his help in preparing photomicrographs, to Mr. Tomokazu Tsutsumi for expert technical assistance and to Dr. Takeshi Nara (Department of Molecular Cell Parasitology, Juntendo University School of

Medicine) for his kind gift of the *S. japonicum* cDNA library. The experimental protocol was approved by the Ethics Review Committee for Animal Experimentation of Kurume University School of Medicine.

References

Beall MJ, Pearce EJ (2001) Human transforming growth factor-beta activates a receptor serine/threonine kinase from the intravascular parasite *Schistosoma mansoni*. J Biol Chem 276:31613–31619

Beall MJ, McGonigle S, Pearce EJ (2000) Functional conservation of *Schistosoma mansoni* Smads in TGF-beta signaling. Mol Biochem Parasitol 111:131–142

Cobbold S, Waldmann, H (1998) Infectious tolerance. Curr Opin Immunol 10:518–524

Cuellar C, Perteguer MJ, Rodero M (2001) Presence of IL-4-like molecules in larval excretory-secretory products and crude extracts from *Anisakis simplex*. Scand J Immunol 53:438–488

Davies SJ, Shoemaker CB, Pearce EJ (1998) A divergent member of the transforming growth factor β receptor family from *Schistosoma mansoni* is expressed on the parasite surface membrane. J Biol Chem 273:11234–11240

Gomez-Escobar N, Van den Biggelaar A, Maizels RM (1997) A member of the TGF-β receptor gene family in the parasitic nematode *Brugia*. Gene 199:101–109

Gomez-Escobar N, Lewis E, Maizels RM (1998) A novel member of the transforming growth factor-β (TGF-β) superfamily from the filarial nematodes *Brugia malayi* and *B. pahangi*. Exp Parasitol 88:200–209

Gomez-Escobar N, Gregory WF, Maizels RM (2000) Identification of tgh-2, a filarial nematode homolog of *Caenorhabditis elegans* daf-7 and human transforming growth factor β, expressed in microfilarial and adult stages of *Brugia malayi*. Infect Immun 68:6402–6410

Grencis RK, Entwistle GM (1997) Production of interferon-gamma homologue by an intestinal nematode: functionally significant or interesting artifact. Parasitology 115:S101-S105

Hirata M, Kage M, Hara T, Nakao M, Fukuma T (1997) Inhibitory effect of circulating egg antigens on *Schistosoma japonicum* egg-induced granuloma formation. J Parasitol 83:842–847

Hirata K, He J, Kuraoka A, Omata Y, Hirata M, Shariful Islam ATM, Noguchi M, Kawabuchi M (2000) Heme oxygenase 1 (HSP-32) is induced in myelin-phagocytosing Schwann cells of injured rat sciatic nerves. Eur J Neurosci 12:4147–4152

Hirata K, He J, Hirakawa Y, Liu W, Wang S, Kawabuchi M (2003) HSP27 is markedly induced in Schwann cell columns and associated regenerating axons. Glia 42:1–11

Hu W, Yan Q, Shen DK, Liu F, Zhu ZD, Song HD, Xu XR, Wang ZJ, Rong YP, Zeng LC, Wu J, Zhang X, Wang JJ, Xu XN, Wang SY, Fu G, Zhang XL, Wang ZQ, Brindley PJ, McManus DP, Xue CL, Feng Z, Chen Z, Han ZG (2003) Evolutionary and biomedical implications of a *Schistosoma japonicum* complementary DNA resource. Nat Genet 35:139–147

Hockley DJ (1973) Ultrastructure of the tegument of *Schistosoma*. Adv Parasitol 11:233–305

Kingsley DM (1994) The TGF-β superfamily: new members, new receptors, and new genetic tests of function in different organisms. Genes Dev 8:133–146

Laemmli UK (1970) Cleavage of structural proteins during the assembly of the head of bacteriophage T4. Nature 227:680–685

Letterio JJ, Roberts AB (1998) Regulation of immune responses by TGF-β. Annu Rev Immunol 16:137–161

Mola PI, Farah OW, Kariuki TM, Nyindo M, Blanton RE, King CL (1999) Cytokine control of the granulomatous response in *Schistosoma mansoni*-infected baboons: role of exposure and treatment. Infect Immun 67:6565–6571

Omer FM, Kurtzhals JA, Riley EM (2000) Maintaining the immunological balance in parasitic infections: a role for TGF-beta? Parasitol Today 16:18–23

Oswald IP, Gazzinelli RT, Sher A, James SL (1992) IL-10 synergizes with IL-4 and transforming growth factor-beta to inhibit macrophage cytotoxic activity. J Immunol 148:3578–3582

Pastrana DV, Raghavan N, Fitzgerald P, Eisinger SW, Metz C, Bucala R, Schleimer RP, Bickel C, Scott AL (1998) Filarial nematode parasites secrete a homologue of the human cytokine macrophage migration inhibitory factor. Infect Immun 66:5955–5963

Pennock JL, Behnke JM, Bickle QD, Devaney E, Grencis RK, Isaac RE, Joshua GW, Selkirk ME, Zhang Y, Meyer DJ (1998) Rapid purification and characterization of L-dopachrome-methylester tautomerase (macrophage-migration-inhibitory factor) from *Trichinella spiralis*, *Trichuris muris* and *Brugia pahangi*. Biochem J 335:495–498

Riddle DL, Albert PS (1997) Genetic and environmental regulation of dauer larva development. In: Riddle DL, Blumenthal T, Meyer BJ, Priess JR (eds) *C. elegans* II. Cold Spring Harbor Laboratory Press, New York, pp 739–768

Takahashi S (1928) On the cercariae of *Schistosoma japonicum*. Katsurada. Okayama Med J 40:1349–1382

Sobhon P, Upatham ES (1990) Snail hosts, life-cycle, and tegumental structure of oriental schistosomes. World Health Organization, Geneva

Verjovski-Almeida S, DeMarco R, Martins EA, Guimarae PE, Ojopi EP, Paquola AC, Piazza JP, Nishiyama MYJr, Kitajima JP, Adamson RE, Ashton PD, Bonaldo MF, Coulson PS, Dillon GP, Farias LP, Gregorio SP, Ho PL, Leite RA, Malaquias LC, Marques RC, Miyasato PA, Nascimento AL, Ohlweiler FP, Reis EM, Ribeiro MA, Sa RG, Stukart GC, Soares MB, Gargioni C, Kawano T, Rodrigues V, Madeira AM, Wilson RA, Menck CF, Setubal JC, Leite LC, Dias-Neto E (2003) Transcriptome analysis of the acoelomate human parasite *Schistosoma mansoni*. Nat Genet 35:148–157

Wahl SM, Frazier-Jessen M, Jin WW, Kopp JB, Sher A, Cheever AW (1997) Cytokine regulation of schistosome-induced granuloma and fibrosis. Kidney Int 51:1370–1375

Williams ME, Caspar P, Oswald I, Sharma HK, Pankewycz O, Sher A, James SL (1995) Vaccination routes that fail to elicit protective immunity against *Schistosoma mansoni* induce the production of TGF-β, which down-regulates macrophage antiparasitic activity. J Immunol 154:4963–4700

Arch Histol Cytol, 68 (1): 29-40 (2005)

The occurrence of nitric oxide synthase-containing axonal baskets surrounding large neurons in rat dorsal root ganglia after sciatic nerve ligation

Wenting Liu, Kazuho Hirata, and Masaru Kawabuchi

Department of Anatomy and Cell Biology, Graduate School of Medical Sciences, Kyushu University, Fukuoka, Japan

Summary. To clarify the possible role of nitric oxide (NO) induced in primary sensory neurons after peripheral axotomy, NO synthase (NOS) immunohistochemistry was carried out on rat L5 dorsal root ganglia after sciatic nerve ligation. The results were compared with the expression of 27-kDa heat shock protein (HSP27), a neuroprotective molecule. In intact animals, NOS-immunoreactive neurons represented about 2% of all dorsal root ganglion (DRG) neurons, whereas HSP27-immunoreactive neurons comprised about 14%. After sciatic nerve ligation, both neurons increased, in number and immunoreactivity, reaching a maximum at 2 weeks, when NOS- and HSP27-immunoreactive neurons represented about 33 and 66%, respectively. NOS-immunoreactive neurons then remained unchanged until 7 weeks although HSP27-immunoreactive neurons showed a slight decline. The increased NOS-immunoreactive neurons were preferentially small (100–500 μm^2) and coexpressed with HSP27 (about 87%). On the other hand, in the proximal stump of sciatic nerves, numerous NOS-immunoreactive fibers with a regenerative profile appeared transiently (2–4 weeks). At higher magnification, an axonal sprout from the NOS-immunoreactive small DRG neurons was found to form a basket-like structure (or basket) mostly around the cell body of NOS-negative large neurons. Retrograde labeling with a fluorescent tracer showed that both neurons sent peripheral axon collaterals to the sciatic nerve. The appearance of this unique structure was most prominent after depletion of the NOS-immunoreactive regenerating fibers in the sciatic nerve (at 7–9 weeks). The findings suggest that NO might be involved in not only axonal regeneration but also the rewiring of two classes of DRG neurons after peripheral nerve injury.

Received October 18, 2004

Address for correspondence: Dr. Kazuho Hirata, Department of Anatomy and Cell Biology, Graduate School of Medical Sciences, Kyushu University, Maidashi 3-1-1, Higashi-ku, Fukuoka, 812-8582 Japan
Tel: +81-92-642-6049, Fax: +81-92-642-6050
E-mail: hirata@anat1.med.kyushu-u.ac.jp

Introduction

Nitric oxide (NO) is an unstable gas that diffuses easily across membranes. It is synthesized from an essential amino acid, L-arginine, by the enzyme NO synthase (NOS) (Bredt and Snyder, 1990), which consists of three different isoforms—the neuronal isoform of NOS (nNOS) in neurons, inducible NOS in macrophages and endothelial NOS in endothelial cells, each being produced by three different genes (for a review see Krumenacker *et al.*, 2004). NO-producing cells are commonly identified by examining the expression of NOS. NOS immunohistochemistry (Zhang *et al.*, 1993; Gonzalez-Hernandez and Rustioni, 1999; Luo *et al.*, 1999; Thippeswamy *et al.*, 2001; Cizkova *et al.*, 2002) and nicotinamide adenine dinucleotide phosphate diaphorase (NADPHd) histochemistry (Fiallos-Estrada *et al.*, 1993), an established method for NOS detection, have shown that nNOS is constitutively expressed in some adult dorsal root ganglion (DRG) neurons, and peripheral axotomy results in a significant increase in NOS-containing neurons in the dorsal root ganglia (DRGs). This finding is consistent with those of in situ hybridization (Verge *et al.*, 1992), RNase protection assays (Luo *et al.*, 1999), and NOS radioassay (Cizkova *et al.*, 2002). As for the role of induced NO in the DRGs after peripheral axotomy, the predominant view is that it has a neuroprotective action

preventing the loss of neurons and facilitating regeneration (Gonzalez-Hernandez and Rustioni, 1999; for a review see Thippeswamy and Morris, 2002). On the other hand, NO is multifunctional (for reviews see Iadicola, 1997 and Krumenacker *et al.*, 2004) and might therefore play other roles: as a neuronal messenger involved in nociceptive transmission (Meller *et al.*, 1992; Choi *et al.*, 1996; Cizkova *et al.*, 2002), and a neurotoxin as reported in avulsed motor neurons (Wu and Li, 1993; Wu *et al.*, 1994; Novikov *et al.*, 1995; Estevez *et al.*, 1998). Thus, the role of the induced NO in axotomized DRG neurons requires further clarification.

The 27-kDa heat shock protein (HSP27) is induced in cells of many types of tissues by stressful stimuli and plays important roles in cellular repair and protective mechanisms (for a review see Ciocca *et al.*, 1993). This protein is reportedly overexpressed in the nervous system under simulated pathological conditions (Kato *et al.*, 1994, 1995; Plumier *et al.*, 1996; Imura *et al.*, 1999; He *et al.*, 2003; Hirata *et al.*, 2003) as well as with serious brain diseases such as Alexander's disease (Iwaki *et al.*, 1993), Alzheimer's disease (Shinohara *et al.*, 1993), and Parkinson's disease (Renkawek *et al.*, 1994). Costigan *et al.* (1998) reported that HSP27 in adult rat DRGs was upregulated after transection of the sciatic nerve—although their study did not focus on changes in HSP27 expression with time. From this finding and the results of their subsequent experiments on neonatal neuronal survival after axotomy *in vivo* and after nerve growth factor (NGF) withdrawal in vitro (Lewis *et al.*, 1999), they concluded that this protein might contribute to cytoskeleton alterations associated with axonal growth and promote the survival of injured sensory neurons. Thus, HSP27 plays a role in neuroprotection in injured or stressed primary sensory neurons and is accordingly a possible marker for these neurons.

To explore the role of NO in injured DRG neurons, the present study immunohistochemically examined alterations of NOS expression in DRGs and the sciatic nerve after ligation, and compared the results with HSP27 expression in DRG neurons. Our data showed a prominent increase in NOS-immunoreactive small DRG neurons, most of which were positive for HSP27, after nerve ligation. The small neurons remained there, even after depletion of the NOS-immunoreactive regenerating fibers in the sciatic nerve, and extended the axonal sprouts which formed a basket-like structure around an NOS-negative large neuron. Further experiments with a retrograde tracer revealed that both of the neurons were axotomized. In addition, the role of *de novo* induced NO in primary sensory neurons was considered.

Materials and Methods

Surgery

Twenty-five adult Wistar rats of both sexes, weighing 180–200 g and aged 6 to 8 weeks, were used for all experiments. After being anesthetized with sodium pentobarbital (50 mg/kg), the proximal one-third of the right sciatic nerve was exposed and tightly ligated with 4-0 silk sutures. The rats were kept alive for 2 and 7 days, and 2, 4, 7 (n=4 at each time point), and 9 weeks (n=3). Two unoperated rats were used as controls.

NOS and HSP27 immunohistochemistry

All animals except those kept alive 9 weeks were deeply anesthetized and transcardially perfused with phosphate buffer saline (PBS) followed by 4% paraformaldehyde in a 0.1 M phosphate buffer (PB), pH 7.4. The L5 DRGs and sciatic nerves on both the operated and unoperated sides were removed and postfixed for 4 h in the same fixative used for perfusion. All materials were put in 30% sucrose in PB for cryoprotection overnight at 4℃, after which 20 μm thick serial sections were cut with a cryostat. The DRG sections were grouped into four parallel series: the first for green fluorescent Nissl staining, the second for single immunofluorescent labeling of HSP27 and fluorescent Nissl staining, the third for double immunofluorescent labeling of HSP27 and NOS, and the fourth for single

Fig. 1. Expression of NOS in longitudinal sections of an intact sciatic nerve used as a control (**A**) and sciatic nerves at 2 days (**B**), 2 weeks (**C**), 4 weeks (**D**) and 7 weeks (**E**) after tight ligation, and enlarged images of the proximal stump at 4 weeks (**F**). NOS-immunoreactive fibers are hardly seen in the intact nerve (**A**), whereas after ligation, a small number appeared in the proximal stump at 2 days (**B**), increasing at 2 (**C**) and 4 weeks (**D**) and then decreasing at 7 weeks (**E**). Note the NOS-immunoreactive fibers extending towards the distal stump alongside the ligature (which shows intense autofluorescence indicated by an asterisk in **D**) at 4 weeks. Higher magnification of the NOS-immunoreactive fibers seen in the proximal stump at 4 weeks shows varicosities and swelling in some regions running retrogradely, suggesting a regenerating profile (**F**). Asterisks in **B**, **C** and **E** show the ligation site. Scale bars=100 μm (A–E), 10 μm (F)